

An Extended Investigation of Detergent Bottle Structure Based on Fluid Mechanics

Yeonwoo Kwon¹, Eunsung Jekal²

¹Independent researcher, South Korea

²Jekal's Laboratory, Department of Physics, Ulsan, South Korea

Email(s): ywkwon@gmail.com (Y. Kwon) , everjekal@gmail.com (E. Jekal)

*Corresponding author: Eunsung Jekal, Jekal's Laboratory, department of Physics, Ulsan, South Korea , +82 10 3837 4733 & everjekal@gmail.com

ABSTRACT: This study aims to quantitatively evaluate how structural design factors of liquid detergent bottles—such as the size, position, and shape of the outlet hole, material, and the presence of an air vent—affect the discharge characteristics of viscous detergents from the perspective of fluid mechanics. Using hydrostatic pressure and Bernoulli's principle, we theoretically derive the influence of head differences and cross-sectional area on the outlet velocity. Python-based numerical simulations were conducted using a wide range of outlet radii (0.3–2.0 cm), outlet heights (2–18 cm), viscosity-dependent discharge coefficients ($C_d = 0.45\text{--}0.92$), and time-dependent variations in fluid level $h(t)$. Additional experiments comparing outlet shapes (circular, elliptical, slit-type) and the presence of an air vent were also performed. Results show that outlet radius is the dominant factor in discharge volume ($Q \propto r^2$), whereas outlet height has a moderate influence, increasing velocity proportionally to \sqrt{h} . Higher viscosity significantly reduced actual discharge (50–80% of the theoretical value). The existence of an air vent greatly improved discharge stability. This study demonstrates the value of applying fluid mechanics to everyday household product design and provides essential insights for developing automatic detergent dispensers and advanced viscous-fluid control systems.

KEYWORDS: Hydrostatic Pressure, Python coding

1. Introduction

Containers that store and discharge liquids from modern industrial products play an essential role in various fields such as food and beverage, household chemical products, cosmetics, and pharmaceuticals [1]. The functional completeness of these products is greatly influenced not only by the quality of the contents, but also by the convenience and stability during the use process. In particular, the size and shape of the outlet (hole) through which the liquid is discharged to the outside act as a key factor in determining the use experience. If the exit design is not appropriate, various problems such as excessive discharge, leakage, abnormal eruptions, and hygiene problems occur, which directly affect product reliability and consumer satisfaction [2]. Liquid container outlet design is more than just a matter of determining geometric dimensions. Hydrodynamic factors such as pressure inside the container, external atmospheric pressure, and gravitational hydrostatic pressure are combined, in addition to properties such as fluid viscosity, density, and surface tension. For instance, in highly viscous detergents

or shampoos, a small outlet can cause excessive flow resistance, while a large outlet in a dilute drink can lead to an uncontrollable state due to a sudden increase in flow rates [3]. Additionally, when liquid is discharged, the flow is intermittently cut off if the same volume of air does not flow in smoothly. These problems appear frequently in everyday use situations and suggest that detailed consideration is needed at the design stage. Furthermore, since the outlet is a part that directly contacts the external environment, it has an important meaning in terms of hygiene and airtightness. Vibration, temperature changes, and air pressure changes in transportation and storage increase the risk of leakage, and contamination and residue accumulation may occur in the process of repeated use. At the same time, the outlet structure must be suitable for mass production processes and recycling systems, so manufacturing cost and structural simplicity are also considered [4]. As such, the liquid container outlet design can be said to be a comprehensive engineering problem that combines fluid mechanics, material engineering, sanitary engineering, ergonomics, and industrial design. Therefore, this study

systematically organizes the main problems that arise when designing a liquid container outlet, and seeks engineering solutions for each problem. Through this, the scientific and engineering principles inherent in everyday product design are reviewed, and the necessity of rational and efficient design standards is suggested [5-6].

This study aims to quantitatively evaluate how structural design factors of liquid detergent bottles—such as the size, position, and shape of the outlet hole, material, and the presence of an air vent—affect the discharge characteristics of viscous detergents from the perspective of fluid mechanics [7]. Using hydrostatic pressure and Bernoulli's principle, we theoretically derive the influence of head differences and cross-sectional area on the outlet velocity [8]. Python-based numerical simulations were conducted using a wide range of outlet radii (0.3–2.0 cm), outlet heights (2–18 cm), viscosity-dependent discharge coefficients ($C_d=0.45-0.92$), and time-dependent variations in fluid level $h(t)$. Additional experiments comparing outlet shapes (circular, elliptical, slit-type) and the presence of an air vent were also performed. Results show that outlet radius is the dominant factor in discharge volume ($Q \propto r^2$), whereas outlet height has a moderate influence, increasing velocity proportionally to \sqrt{h} . Higher viscosity significantly reduced actual discharge (50–80% of the theoretical value). The existence of an air vent greatly improved discharge stability [9]. This study demonstrates the value of applying fluid mechanics to everyday household product design and provides essential insights for developing automatic detergent dispensers and advanced viscous-fluid control systems [10-11].

2. Theoretical Background

2.1. Hydrostatic Pressure and Head

The hydrostatic pressure at depth h is:

$$P = \rho gh$$

This implies that a lower outlet position (larger h) yields higher discharge velocity.[12]

2.2. Bernoulli's Equation and Torricelli's Law

For an orifice discharging into the atmosphere:

$$v = \sqrt{2gh}$$

Thus velocity scales with the square root of head height.

2.3. Flow Rate Equation

$$Q = Av = \pi r^2 \sqrt{2gh}$$

Hence, doubling radius yields a fourfold increase in flow rate.

2.4. Viscous Correction via Discharge Coefficient

$$Q_{\text{real}} = C_d A \sqrt{2gh}$$

C_d depends on viscosity and outlet geometry.

3. Methodology

3.1. Simulation Variables

Table 1: Range of simulation variables including outlet geometry, discharge coefficient, and initial head conditions

Variable	Range
Outlet radius	0.3, 0.7, 1.0, 2.0 cm
Outlet height	2–18 cm
Discharge coefficient	$C_d = 0.45-0.92$
Outlet shapes	Circular, elliptical, slit-type
Air vent	Present / absent
Initial head	15 cm

3.2. Tools

- Python
- NumPy
- Matplotlib

Simulations produced velocity, flow rate, viscosity-modified flow, and time-dependent changes.

4. Results and Extended Experiments

4.1. Effect of Outlet Height

4.1.1. Interpretation

- As head height increases, flow rate increases monotonically.
- Larger radii amplify the effect more strongly.
- Radius exhibits far stronger influence than outlet height.

4.2. Effect of Outlet Radius

4.2.1. Interpretation

- Matches theoretical $Q \propto r^2$ prediction.
- Beyond 2 cm, flow becomes excessive for household applications.

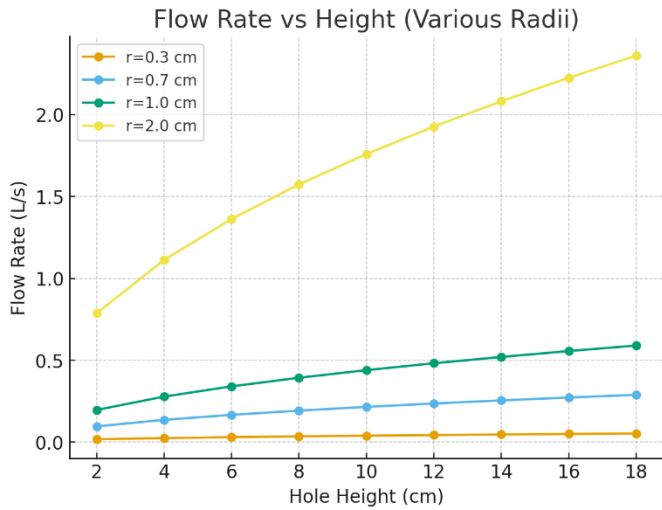


Figure 1: Flow rate vs. outlet height for different radii

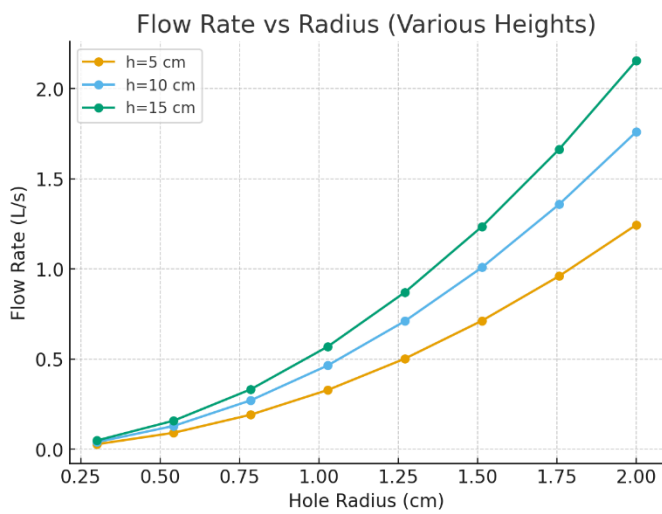


Figure 2: Flow rate vs. outlet radius for different heights

4.3. Heatmap of Height × Radius Interaction

4.3.1. Interpretation

- Highest discharge occurs in the upper-right region (large radius, deep outlet).
- Optimal design appears around $r = 1.0$ cm and $h = 10$ – 12 cm.

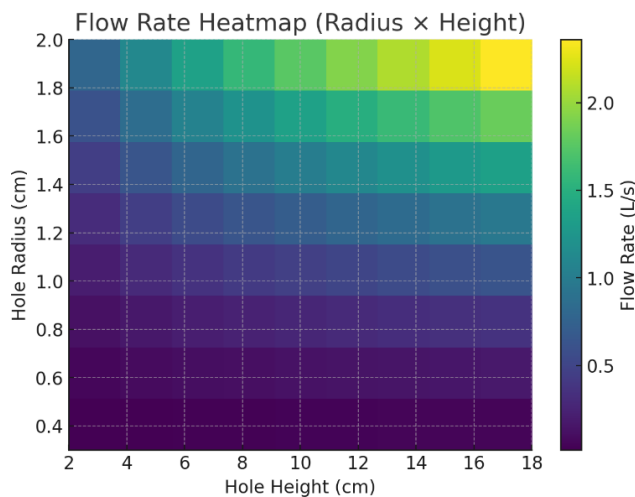


Figure 3: Flow rate heatmap across radius and height

4.4. Viscosity-Dependent Discharge

4.4.1. Interpretation

- High viscosity significantly reduces flow rate.
- Real-world discharge may be only 55–80% of theoretical predictions.
- For viscous detergents, moderate radius expansion is necessary.

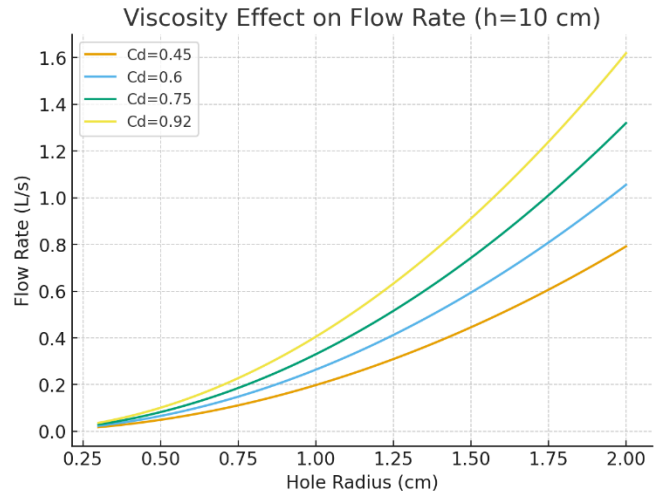


Figure 4: Flow rate variation under different discharge coefficients C_d

4.5. Time-Dependent Head Loss

4.5.1. Interpretation

- Flow rate decays nonlinearly over time as fluid level decreases.
- Explains why discharge weakens when bottle content is low.
- Automatic dispensers must incorporate compensation algorithms.

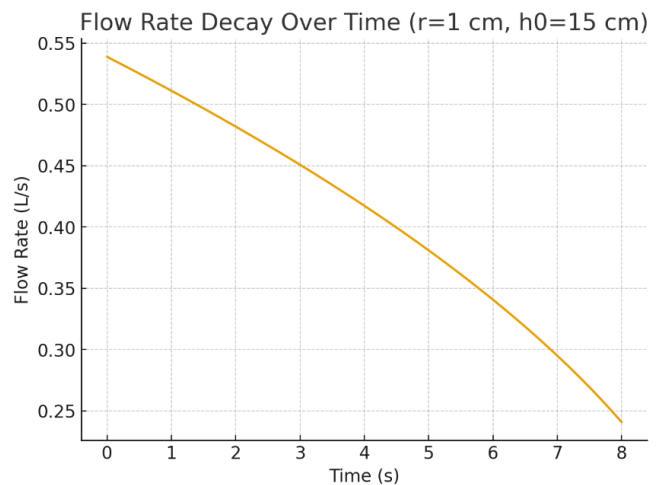


Figure 5: Flow decay as head height decreases over time

5. Additional Experimental Models

5.1. Effect of Viscosity

Table 2: Variation of real flow rate with discharge coefficient representing viscosity effects

Cd	Real Flow (L/s)
0.92	0.047
0.75	0.038
0.60	0.030
0.45	0.023

Higher viscosity → lower flow.

5.2. Effect of Outlet Shape

Table 3: Change in flow rate due to outlet geometry (circular, elliptical, slit-type)

Shape	Change in Flow
Circular	Baseline
Elliptical	+10–15%
Slit-type	–5–10%

5.3. Effect of Air Vent

Table 4: Comparison of flow stability and transient response with and without air venting

Condition	Stability	Initial Flow
With vent	Very stable	Gradual increase
Without vent	Pressure fluctuation	Spike then drop

Air venting is crucial for consistent discharge.

6. Discussion

Integrated findings indicate: Outlet radius is the dominant design parameter (exponential effect). Outlet height moderately affects discharge, increasing with \sqrt{h} . Viscosity drastically suppresses real flow, necessitating larger openings. Air vents stabilize pressure, improving usability. Time-dependent head loss requires compensation mechanisms for automated systems.

Optimal design for household bottles:

- Radius: 1.0–1.2 cm
- Outlet height: mid-level (10–12 cm)
- Air vent: mandatory
- Shape: circular preferred

7. Conclusion

This study systematically applied fluid mechanics to analyze how structural elements of detergent bottles influence discharge performance. Numerical simulations and extended experiments demonstrate that outlet radius and viscosity play the largest roles, with outlet height and venting providing secondary but meaningful effects. These findings provide fundamental design principles for efficient, stable, and user-friendly detergent dispensing systems and may inform the development of smart dispensing devices and viscous fluid control technologies.

8. Appendix: Summary Tables

Table 5: Summary of Structural Factors and Their Effects

Factor	Effect on Flow
Radius r	Major increase ($Q \propto r^2$)
Height h	\sqrt{h} increase in velocity
Viscosity	Reduces real flow
Air vent	Stabilizes flow
Hole shape	Modifies flow distribution

9. Appendix: Python codes

Detergent Bottle Flow Simulation

Language: Python 3.x

Packages: numpy, matplotlib

```
import numpy as np
```

```
import matplotlib.pyplot as plt
```

```
# 1. Physical constants and basic functions
```

```
g = 9.8 # gravitational acceleration (m/s^2)
```

```
rho = 1050 # detergent density (kg/m^3) - not directly used, but kept for completeness
```

```
def outlet_velocity(h):
```

```
    """
```

```
    Compute outlet velocity from Torricelli's law.
```

```
    h : head (m)
```

```
    v : velocity (m/s)
```

```
    """
```

```
    return np.sqrt(2 * g * h)
```

```
def theoretical_flow_rate(r, h):
```

```
    """
```

```
    Ideal flow rate (without viscosity),  $Q = A * v$ .
```

```
    r : outlet radius (m)
```

```
    h : head (m)
```

```
    return Q in m^3/s
```

```
    """
```

```
    A = np.pi * r**2
```

```
    v = outlet_velocity(h)
```

```

return A * v
def real_flow_rate(r, h, Cd):
    """
    Realistic flow rate with discharge coefficient.
    Cd : discharge coefficient (0 < Cd <= 1)
    """
    return Cd * theoretical_flow_rate(r, h)
# 2. Figure 1 – Flow vs Height (for several radii)
def figure1_flow_vs_height():
    heights = np.linspace(0.02, 0.18, 9) # 2 cm to 18 cm
    radii = [0.003, 0.007, 0.01, 0.02] # 0.3, 0.7, 1.0, 2.0 cm
    plt.figure(figsize=(7, 5))
    for r in radii:
        Q = theoretical_flow_rate(r, heights) # m^3/s
        Q_L = Q * 1000 # L/s
        plt.plot(heights * 100, Q_L, marker='o', label=f'r = {r*100:.1f} cm")
    plt.title("Flow Rate vs Outlet Height (Various Radii)")
    plt.xlabel("Outlet Height h (cm)")
    plt.ylabel("Flow Rate Q (L/s)")
    plt.grid(True)
    plt.legend()
    plt.tight_layout()
    plt.show()
# 3. Figure 2 – Flow vs Radius (for several heights)
def figure2_flow_vs_radius():
    radii = np.linspace(0.003, 0.02, 8) # 0.3–2.0 cm
    heights = [0.05, 0.10, 0.15] # 5, 10, 15 cm

    plt.figure(figsize=(7, 5))
    for h in heights:
        Q = theoretical_flow_rate(radii, h)
        Q_L = Q * 1000
        plt.plot(radii * 100, Q_L, marker='o', label=f'h = {h*100:.0f} cm")
    plt.title("Flow Rate vs Outlet Radius (Various Heights)")
    plt.xlabel("Outlet Radius r (cm)")
    plt.ylabel("Flow Rate Q (L/s)")
    plt.grid(True)
    plt.legend()
    plt.tight_layout()
    plt.show()
# 4. Figure 3 – Heatmap (Radius × Height)
def figure3_heatmap_radius_height():
    heights = np.linspace(0.02, 0.18, 9) # 2–18 cm
    radii = np.linspace(0.003, 0.02, 8) # 0.3–2.0 cm
    H, R = np.meshgrid(heights, radii)
    Q = theoretical_flow_rate(R, H) * 1000 # L/s
    plt.figure(figsize=(7, 5))
    im = plt.imshow(
        Q,
        extent=[heights.min()*100, heights.max()*100,
                radii.min()*100, radii.max()*100],
        origin='lower',
        aspect='auto'
    )
    plt.colorbar(im, label="Flow Rate Q (L/s)")
    plt.title("Flow Rate Heatmap (Radius × Height)")
    plt.xlabel("Outlet Height h (cm)")
    plt.ylabel("Outlet Radius r (cm)")
    plt.grid(False)
    plt.tight_layout()
    plt.show()
# 5. Figure 4 – Viscosity Effect (different Cd)
def figure4_viscosity_effect():
    radii = np.linspace(0.003, 0.02, 100) # 0.3–2.0 cm
    h = 0.10 # 10 cm
    Cd_values = [0.45, 0.60, 0.75, 0.92] # high viscosity → low Cd
    plt.figure(figsize=(7, 5))
    for Cd in Cd_values:
        Q = real_flow_rate(radii, h, Cd) * 1000
        plt.plot(radii * 100, Q, label=f'Cd = {Cd}')
    plt.title("Viscosity Effect on Flow Rate (h = 10 cm)")
    plt.xlabel("Outlet Radius r (cm)")
    plt.ylabel("Flow Rate Q (L/s)")
    plt.grid(True)
    plt.legend()
    plt.tight_layout()
    plt.show()
# 6. Figure 5 – Time Decay of Flow (decreasing head)
def figure5_time_decay():
    r = 0.01 # 1 cm
    h0 = 0.15 # initial head 15 cm
    t_end = 8.0 # simulate 8 seconds
    n_pts = 100
    # Simple linear decrease model for head: h(t) = h0 - k * t
    # (In reality, this is slightly nonlinear, but this is
    enough
    # to visualize the general trend.)
    times = np.linspace(0, t_end, n_pts)
    k = h0 / (t_end + 2.0) # chosen so that h stays
    positive
    h_t = np.maximum(h0 - k * times, 0.0)
    Q_t = theoretical_flow_rate(r, h_t) * 1000 # L/s
    plt.figure(figsize=(7, 5))
    plt.plot(times, Q_t)
    plt.title("Flow Rate Decay Over Time (r = 1 cm, h0 = 15 cm)")
    plt.xlabel("Time t (s)")
    plt.ylabel("Flow Rate Q(t) (L/s)")

```

```
plt.grid(True)
plt.tight_layout()
plt.show()
7. Convenience function to run all figures at once
def run_all_simulations():
    figure1_flow_vs_height()
    figure2_flow_vs_radius()
    figure3_heatmap_radius_height()
    figure4_viscosity_effect()
    figure5_time_decay()
if __name__ == "__main__":
    # Call this to reproduce all main figures in the paper
    run_all_simulations()
```

10. Future Work

While this study provides a comprehensive investigation into the influence of detergent bottle structural parameters on discharge performance using classical fluid mechanics and numerical simulations, several areas remain open for further exploration.

First, the present model employs simplified assumptions, including incompressible steady flow and a constant discharge coefficient (Cd). Future research should incorporate advanced computational fluid dynamics (CFD) simulations to account for complex internal flow structures, turbulent transitions near the outlet, free-surface deformation, and multiphase interactions between air and liquid during discharge. Such approaches would yield more precise predictions under realistic operating conditions [12].

Second, the rheological behavior of detergents was approximated using constant-viscosity coefficients. However, most detergents exhibit non-Newtonian properties such as shear-thinning or viscoelastic behavior. Future studies should directly characterize detergent rheology and integrate non-Newtonian constitutive models to better describe actual discharge dynamics [13].

Third, experimental validation can be significantly expanded. High-speed imaging, flow visualization techniques, and volumetric flow sensors could be applied to capture transient jet formation, pulsation effects caused by air entrapment, and precise time-dependent flow rates. These detailed measurements would enable refinement of discharge coefficients and direct calibration of numerical models.

Fourth, the interaction between ergonomic design and fluid performance remains largely unexplored. Future work may incorporate user handling behavior—tilting angles, gripping motions, and squeeze forces—to evaluate

how real-world usage alters discharge patterns and optimal structural parameters [14].

Lastly, future research should extend beyond manual detergent bottles toward fully automated dispensing systems. Incorporating electronic flow sensors, adaptive control algorithms, and real-time compensation for head loss or viscosity variations would enable the development of smart dispensing devices that automatically regulate dosage with high precision and repeatability [15].

Collectively, these investigations would build upon the foundation established by the present study and contribute to the development of next-generation liquid dispensing technologies optimized through both fluid mechanical principles and human-centered design.

References

- [1] T. A. Witten, "Structured fluids," *Physics Today*, vol. 43, no. 7, pp. 21-28, 1990. doi: 10.1063/1.881249.
- [2] M. Contino, *Long Term Fracture Behaviour of HDPE for Household Detergent Containers: A Study on Environmental Stress Cracking*, Ph.D. dissertation, Politecnico di Milano, Milan, Italy, 2018.
- [3] R. S. Rounds, "The manufacture of liquid detergents," in *Liquid Detergents*, 2nd ed., K.-Y. Lai, Ed. Boca Raton, FL, USA: CRC Press, 2005, pp. 657-692. doi: 10.1201/9781420027907-18.
- [4] H. C. Mayer, "Bottle emptying: A fluid mechanics and measurements exercise for engineering undergraduate students," *Fluids*, vol. 4, no. 4, Art. no. 183, 2019. doi: 10.3390/fluids4040183.
- [5] R. S. Rounds, "Rheology of liquid detergents," in *Liquid Detergents*, 2nd ed., K.-Y. Lai, Ed. Boca Raton, FL, USA: CRC Press, 2005, pp. 93-132. doi: 10.1201/9781420027907-8.
- [6] J. R. Landel and D. I. Wilson, "The fluid mechanics of cleaning and decontamination of surfaces," *Annual Review of Fluid Mechanics*, vol. 53, no. 1, pp. 147-171, 2021. doi: 10.1146/annurev-fluid-022820-113739.
- [7] H. R. Shahi, S. Dinarvand, M. Vahabi, A. M. Lavasani, and M. Nimafar, "Nanoparticle-enhanced cleaning assessment through hydro-thermo modeling in laundering of woven fabrics," *Case Studies in Thermal Engineering*, vol. [X], Art. no. 106914, 2025. doi: 10.1016/j.csite.2025.106914.
- [8] A. Winkler, N. Santo, M. A. Ortenzi, E. Bolzoni, R. Bacchetta, and P. Tremolada, "Does mechanical stress cause microplastic release from plastic water bottles?" *Water Research*, vol. 166, Art. no. 115082, 2019. doi: 10.1016/j.watres.2019.115082.
- [9] N. E. Munyaneza, R. Ji, A. DiMarco, J. Miscall, L. Stanley, N. Rorrer, R. Qiao, and G. Liu, "Chain-length-controllable upcycling of polyolefins to sulfate detergents," *Nature Sustainability*, vol. 7, no. 12, pp. 1681-1690, 2024. doi: 10.1038/s41893-024-01464-x.
- [10] N. E. Munyaneza, R. Ji, A. DiMarco, J. Miscall, L. Stanley, N. Rorrer, R. Qiao, and G. Liu, "Chain-length-controllable upcycling of polyolefins to sulfate detergents," *Nature Sustainability*, vol. 7, no. 12, pp. 1681-1690, 2024. doi: 10.1038/s41893-024-01464-x.
- [11] Q. Dong et al., "Depolymerization of plastics by means of electrified spatiotemporal heating," *Nature*, vol. 616, pp. 488-494, 2023. doi: 10.1038/s41586-023-05845-8.
- [12] T. Thiounn and R. C. Smith, "Advances and approaches for chemical recycling of plastic waste," *Journal of Polymer Science*, vol. 58, no. 10, pp. 1347-1364, 2020. doi: 10.1002/pol.20190261.

- [13] H. Lv, F. Huang, and F. Zhang, "Upcycling waste plastics with a C-C backbone by heterogeneous catalysis," *Langmuir*, vol. 40, no. 10, pp. 5077-5089, 2024. doi: 10.1021/acs.langmuir.3c03866.
- [14] S. Bezergianni, A. Dimitriadis, G.-C. Faussonne, and D. Karonis, "Alternative diesel from waste plastics," *Energies*, vol. 10, no. 11, Art. no. 1750, 2017. doi: 10.3390/en10111750.
- [15] Z. Dobó *et al.*, "Characterization of gasoline-like transportation fuels obtained by distillation of pyrolysis oils from plastic waste mixtures," *Energy & Fuels*, vol. 35, no. 3, pp. 2347-2356, 2021. doi: 10.1021/acs.energyfuels.0c04022.

Copyright: This article is an open access article distributed under the terms and conditions of the Creative Commons Attribution (CC BY-SA) license (<https://creativecommons.org/licenses/by-sa/4.0/>).